

differences in the efficiencies of this decay due to differences in the amount of metal character present in the excited state. The smaller the CT character, the stronger the spin-orbit coupling effects and the more efficient the decay. Nonradiative decay pathways in the complexes showing both fluorescence and phosphorescence are more complicated. However the trend in the phosphorescence lifetimes for the compounds studied reflects the predicted trend in the CT character of the emitting state. The compounds with the largest CT character have the longest phosphorescence lifetimes.

Summary

The electronic absorption and emission spectra of a series of $\text{Re}(\text{CO})_8(\alpha, \alpha'\text{-diimine})$ compounds under various conditions were measured and analyzed. The broad, intense, lowest energy absorption band from these compounds is assigned to a composite of several metal to π_1^* (α, α' -diimine) charge-transfer transitions

including two $d\pi \rightarrow \pi_1^*$ transitions, a $d\delta \rightarrow \pi_1^*$ transition, and possibly a $\sigma_b(\text{Re-Re}) \rightarrow \pi_1^*$ transition. Emission from these compounds, is assigned to a $\text{Re } d \rightarrow \pi_1^*$ MLCT excited state. $\text{Re}_2(\text{CO})_8(2,2'\text{-bpy})$, $\text{Re}_2(\text{CO})_8(4,4'\text{-Me}_2\text{bpy})$, $\text{Re}_2(\text{CO})_8(1,10\text{-phen})$, and $\text{Re}_2(\text{CO})_8(\text{isopr-Pyca})$ exhibit both fluorescence and phosphorescence from this excited state, whereas only phosphorescence is observed from $\text{Re}_2(\text{CO})_8(\text{isopr-DAB})$ and $\text{Re}_2(\text{CO})_8(\text{ptol-DAB})$.

Acknowledgment. This work was supported by the National Science Foundation (Grant CHE 88-06775). We thank Professor Nancy Haegel and Mr. Vince Mazzi for their assistance in measuring the near-infrared emission spectra.

Registry No. $\text{Re}_2(\text{CO})_8(2,2'\text{-bpy})$, 130404-88-5; $\text{Re}_2(\text{CO})_8(4,4'\text{-Me}_2\text{bpy})$, 130327-18-3; $\text{Re}_2(\text{CO})_8(1,10\text{-phen})$, 130404-89-6; $\text{Re}_2(\text{CO})_8(\text{isopr-Pyca})$, 130327-19-4; $\text{Re}_2(\text{CO})_8(\text{isopr-DAB})$, 97698-45-8; $\text{Re}_2(\text{CO})_8(\text{p-tol-DAB})$, 99791-93-2.

Contribution from the Department of Chemistry, Gorlaeus Laboratoria, P.O. Box 9502, 2300 RA Leiden, The Netherlands, Anorganisch Chemisch Laboratorium, University of Amsterdam, Nieuwe Achtergracht 166, 1018 WV Amsterdam, The Netherlands, and School of Chemical Sciences, Dublin City University, Dublin 9, Ireland

pH Control of the Photophysical Properties of Ruthenium Complexes Containing 3-(Pyrazin-2-yl)-1,2,4-triazole Ligands

Heleen A. Nieuwenhuis,[†] Jaap G. Haasnoot,^{*,†} Ronald Hage,[†] Jan Reedijk,[†] Theo L. Snoeck,[‡] Derk J. Stufkens,[‡] and Johannes G. Vos[§]

Received January 11, 1990

A new series of $[\text{Ru}(\text{bpy})_2(\text{L})](\text{PF}_6)_2$ complexes, where bpy = 2,2'-bipyridine and L = 3-(pyrazin-2-yl)-1,2,4-triazole (HL0), 1-methyl-3-(pyrazin-2-yl)-1,2,4-triazole (L1), 1-methyl-5-(pyrazin-2-yl)-1,2,4-triazole (L2), and 3-methyl-5-(pyrazin-2-yl)-1,2,4-triazole (L3), have been prepared and characterized. ¹H NMR spectroscopy has been used to analyze the coordination modes of the ligands, while UV-vis absorption, emission, and resonance Raman spectroscopies, together with electrochemistry, have been used to study the properties of the complexes in their ground and excited states. Electrochemical data and resonance Raman experiments show that in the compounds containing protonated or *N*-methyl-substituted pyrazinyltriazole ligands the lowest π^* levels are pyrazinyltriazole based, while for the complexes with deprotonated ligands the lowest π^* levels are located on the bpy ligands. Furthermore, the emission data (lifetimes and maxima) suggest that the emitting states can be changed from bpy to pyrazinyltriazole based upon lowering the pH for $[\text{Ru}(\text{bpy})_2(\text{L0})]^+$ and $[\text{Ru}(\text{bpy})_2(\text{L3})]^+$. Another interesting feature is that the absorption and emission maxima of $[\text{Ru}(\text{bpy})_2(\text{L0})]^+$ and $[\text{Ru}(\text{bpy})_2(\text{L3})]^+$ do not change to a large extent when the pH is lowered.

Introduction

Much work carried out in the field of ruthenium coordination chemistry has revealed that ruthenium compounds with nitrogen-containing ligands have interesting electrochemical, photophysical, and photochemical properties. In particular, compounds such as $[\text{Ru}(\text{bpy})_3]^{2+}$ (bpy = 2,2'-bipyridine) and $[\text{Ru}(\text{bpz})_3]^{2+}$ (bpz = 2,2'-bipyrazine) have been investigated in detail and have been suggested as potential catalysts for the conversion of solar energy.¹⁻³

We are at present investigating the effect of asymmetry in bidentate ligands on the physical properties of ruthenium and osmium compounds, and in earlier papers we reported ruthenium compounds containing 3-(pyridin-2-yl)-1,2,4-triazoles.^{4,5} By the combination of a six- and a five-membered ring into a bidentate ligand, two different kinds of coordinating nitrogen atoms are created. As it is known that five-membered rings, as for example 1,2,4-triazoles, pyrazoles, and imidazoles, are strong σ -donor ligands and weak π -acceptor ligands compared to 2,2'-bipyridine, it is anticipated that asymmetric bidentate ligands of this kind may produce ruthenium compounds with unusual excited-state properties. This paper describes both the preparation of some novel pyrazinyltriazole ligands and the physical properties of a series of ruthenium bis(bipyridine) complexes containing these ligands.

From experiments described in the literature,⁶ it is known that bipyrazine has weaker σ -donor capacities and stronger π -acceptor properties than bipyridine. It is, therefore, expected that there will be substantial differences between the photophysical properties of the compounds containing pyridyltriazoles and pyrazinyltriazoles. Of particular interest to us is the nature of the lowest unoccupied molecular orbital (LUMO) in these compounds. An additional feature of pyrazine-containing ligands is the possibility of protonation of the noncoordinating pyrazine atom in strong acidic media.⁷⁻⁹

Experimental Section

Physical Methods. ¹H NMR spectra were obtained on a JEOL JNM-FX 200 MHz spectrometer, while the COSY ¹H NMR spectra were recorded on a Bruker 300-MHz spectrometer, as reported previously.¹⁰ The measurements of the ligands were carried out in CDCl₃,

- (1) Dürr, H.; Dörr, G.; Zengerle, K.; Mayer, E.; Curchod, J. H.; Braun, A. *M. Nouv. J. Chim.* **1985**, *9*, 717.
- (2) Crutchley, R. J.; Lever, A. B. P. *J. Am. Chem. Soc.* **1980**, *102*, 7129.
- (3) Juris, A.; Balzani, V.; Barigelletti, F.; Campagna, S.; Belsler, P.; von Zelewsky, A. *Coord. Chem. Rev.* **1988**, *84*, 85.
- (4) Long, C.; Vos, J. G. *Inorg. Chim. Acta* **1984**, *89*, 125.
- (5) Hage, R.; Prins, R.; Haasnoot, J. G.; Reedijk, J.; Vos, J. G. *J. Chem. Soc., Dalton Trans.* **1987**, 1389.
- (6) Crutchley, R. J.; Lever, A. B. P. *Inorg. Chem.* **1982**, *21*, 2277.
- (7) Crutchley, R. J.; Kress, N.; Lever, A. B. P. *J. Am. Chem. Soc.* **1983**, *105*, 1170.
- (8) Bond, A.; Haga, M. *Inorg. Chem.* **1986**, *25*, 4507.
- (9) Kirsch-De Mesmaeker, A.; Jacquet, L.; Nasielski, J. *Inorg. Chem.* **1988**, *27*, 4451.
- (10) Hage, R.; Dijkhuis, A. H. J.; Haasnoot, J. G.; Prins, R.; Reedijk, J.; Buchanan, B. E.; Vos, J. G. *Inorg. Chem.* **1988**, *27*, 2185.

[†]Gorlaeus Laboratoria.

[‡]University of Amsterdam.

[§]Dublin City University.

Table I. ^1H NMR Chemical Shifts (CDCl_3 in ppm Relative to TMS) and Electrochemical Data (CH_3CN with 0.1 M TBAP in V vs SCE) of the Free Pyrazinyltriazole Ligands

	pyrazine ring			triazole ring		redn pot.
	H_3	H_5	H_6	H_5'	CH_3	
HL0	9.46 (d)	8.70 (2 d)	8.66 (d)	8.25 (s)		-1.35
L1	9.39 (d)	8.69 (2 d)	8.62 (d)	8.22 (s)	4.06 (s)	-1.97
L2	9.29 (d)	8.80 (2 d)	8.77 (d)	8.12 (s)	4.23 (s)	-1.23
HL3	9.20 (d)	8.71 (2 d)	8.67 (d)		2.41 (s)	-1.49
bpz	9.53 (d)	8.84				-1.76 ⁴¹
bpy						-2.21 ³⁷

and the coordination compounds were measured in $(\text{CD}_3)_2\text{CO}$.

UV-vis measurements were carried out on a Perkin-Elmer 330 or on a Shimadzu UV-240 spectrophotometer, using matched 1-cm quartz cells. Titrations in the pH range from 1 to 10 were carried out in a Britton-Robinson buffer solution (0.04 M H_3BO_4 , 0.04 M H_3PO_4 , 0.04 M H_3CCOOH). Titrations in the pH range from 3 to -5 were carried out by the use of concentrated sulfuric acid.

High-performance liquid chromatography was carried out by using a Waters 990 photodiode-array HPLC system in conjunction with an NEC APC III computer, a Waters Model 6000 A pump, a 20- μL injector loop, and a μ Partisil SCX radial PAK cartridge. The detection wavelength used was 280 nm. The chromatography was carried out by using acetonitrile/water (80/20) containing 0.08 M LiClO_4 as a mobile phase. The flow rate used was 3 mL/min.

Cyclic voltammograms (CV) and differential-pulse polarograms (DPP) were recorded on an EG&G Par C Model 303 potentiostat with an EG&G Par 384B polarographic analyzer. Measurements were carried out in HPLC grade acetonitrile by using 0.1 M tetrabutylammonium perchlorate (TBAP) as electrolyte. The scan rate for the cyclic voltammograms was 100 mV/s and that for the differential-pulse measurements 4 mV/s with a peak height of 20 mV.

Emission spectra were recorded on a Perkin-Elmer MPF-44B luminescence spectrometer using a Hamamatsu R928 red-sensitive detector and an emission slit width of 10 nm at room temperature and 2.5 nm at 77 K; spectra were not corrected for photomultiplier response. The lifetime measurements were carried out on a modified Applied Photo-physics single-photon instrument. At room temperature the measurements were carried out in acetonitrile, and at low temperature measurements were carried out in a mixture of distilled propionitrile/butyronitrile (4/5 v/v).

Resonance Raman spectra were recorded in ethanol solution by using a spinning cell and a Jobin Yvon HG2S Ramanor spectrophotometer. The samples were excited by an SP Model 171 argon ion laser. Excitation took place at 458, 488, and 514.5 nm.

Elemental analyses were carried out at University College, Dublin.

Preparation of the Ligands. Cyanopyrazine was prepared according to literature methods.¹¹

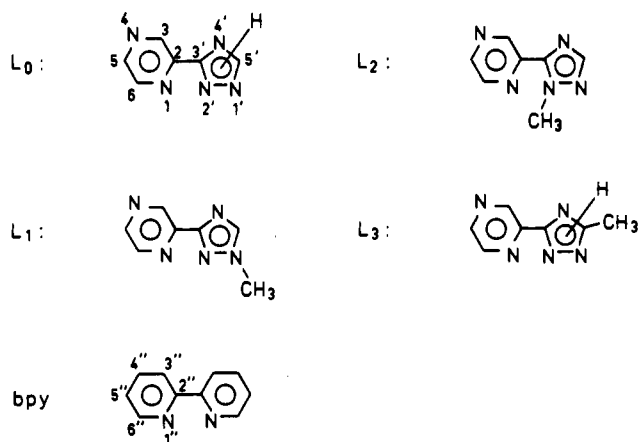
The pyrazinyltriazole ligands were prepared as reported in the literature for analogous 3-(pyridin-2-yl)-1,2,4-triazoles.¹²⁻¹⁴

Preparation of Pyrazinamidrazone. A 20-mL volume of ethanol was added to a mixture of 5.0 g (0.048 mol) of molten 2-cyanopyrazine and an equimolar amount of 2.4 g of hydrazine hydrate. For the synthesis of 1-methyl-3-(pyrazin-2-yl)-1,2,4-triazole an equimolar amount of methylhydrazine was used. The solution was stirred for 1 h at room temperature. Yellow crystals were collected by filtration.

Preparation of the Ligands 3-(Pyrazin-2-yl)-1,2,4-triazole (HL0), 1-Methyl-3-(pyrazin-2-yl)-1,2,4-triazole (L1), and 3-Methyl-5-(pyrazin-2-yl)-1,2,4-triazole (HL3). The pyrazinamidrazone (14 g; 100 mmol) was dissolved in an 10-fold excess of cold formic acid at temperatures below 10 °C. For the synthesis of 3-methyl-5-(pyrazin-2-yl)-1,2,4-triazole, acetic acid was used instead of formic acid. Upon addition of the amidrazone, the mixture was stirred for 3 h at room temperature. After subsequent heating to dryness at 120 °C, the ligand crystallized out. The ligands were recrystallized from ethanol. HL0: yield 48%; mp 213 °C. L1: yield 50%; mp 173 °C. HL3: yield 64%; mp 246 °C.

The ^1H NMR and electrochemical data of the free ligands are given in Table I, and the structures are shown in Figure 1.

Preparation of 1-Methyl-5-(pyrazin-2-yl)-1,2,4-triazole (L2). A 4.2-g (0.034-mol) amount of pyrazinamide was dissolved in 12.4 g (0.104 mol) of *N,N*-dimethylformamide dimethyl acetal while the solution was heated

**Figure 1.** Structural formula of the ligands HL0, L1, L2, and HL3 (with numbering for NMR spectroscopy).

to 70 °C. After the mixture was cooled at -20 °C yellow crystals of pyrazinylformamidine were collected by filtration and washed with cold diethyl ether.

To a solution of 1.0 g (0.024 mol) of methylhydrazine in 40 mL of acetic acid was added 3.6 g (0.022 mol) of pyrazinylformamidine. After the mixture was heated at reflux for 1.5 h, the acetic acid was evaporated under reduced pressure to produce an oil, which was dissolved in chloroform.

The chloroform solution was neutralized with sodium bicarbonate, washed with water, and dried over sodium sulfate. After filtration the chloroform was removed under reduced pressure and the residue was dissolved in diethyl ether. Upon cooling of the solution to -20 °C, the ligand crystallized. The ligand was recrystallized from absolute ethanol. L2: yield 22%; mp 82 °C.

The ^1H NMR and electrochemical data obtained for the ligand are given in Table I.

Preparation of the Complexes. $[\text{Ru}(\text{bpy})_2(\text{L})]^{2+}$ compounds were prepared according to literature methods.¹⁵

A 1-mmol (0.51-g) amount of $[\text{Ru}(\text{bpy})_2\text{Cl}_2]^{16}$ and an excess of ligand L (1.5-2 mmol; 0.2-0.3 g) were refluxed in 50 mL of ethanol for 8 h. The solvent was evaporated, and the residue was dissolved in a small amount of water. The complexes were precipitated with ammonium hexafluorophosphate. Recrystallization took place in a mixture of 1/1 acetone and water. To obtain the compound containing L0, one drop of 10% ammonium hydroxide was added, to ensure the formation of the pure deprotonated complex.

$[\text{Ru}(\text{bpy})_2(\text{L0})(\text{PF}_6)_2 \cdot \text{H}_2\text{O}$. Yield: 0.23 g (30%). Anal. Calcd for $\text{C}_{26}\text{H}_{22}\text{F}_6\text{N}_9\text{OPRu}$: C, 44.3; H, 2.9; N, 17.9; P, 4.4. Found: C, 43.6; H, 3.1; N, 17.3; P, 4.2.

$[\text{Ru}(\text{bpy})_2(\text{L1})(\text{PF}_6)_2 \cdot 2\text{H}_2\text{O}$. Yield: 0.54 g (71%). Anal. Calcd for $\text{C}_{27}\text{H}_{27}\text{F}_{12}\text{N}_9\text{O}_2\text{P}_2\text{Ru}$: C, 36.0; H, 3.0; N, 14.0; P, 6.9. Found: C, 36.1; H, 2.8; N, 13.7; P, 6.7.

$[\text{Ru}(\text{bpy})_2(\text{L2})(\text{PF}_6)_2$. Yield: 0.43 g (60%). Anal. Calcd for $\text{C}_{27}\text{H}_{23}\text{F}_{12}\text{N}_9\text{P}_2\text{Ru}$: C, 37.5; H, 2.7; N, 14.6; P, 7.2. Found: C, 37.9; H, 2.7; N, 14.2; P, 7.6.

$[\text{Ru}(\text{bpy})_2(\text{HL3})(\text{PF}_6)_2 \cdot 2\text{H}_2\text{O}$. Yield: 0.42 g (58%). Anal. Calcd for $\text{C}_{27}\text{H}_{27}\text{F}_{12}\text{N}_9\text{O}_2\text{P}_2\text{Ru}$: C, 36.0; H, 3.0; N, 14.0; P, 6.9. Found: C, 36.7; H, 3.1; N, 13.7; P, 6.7.

$[\text{Ru}(\text{L1})_3](\text{PF}_6)_2$ was prepared by refluxing 1 mmol of RuCl_3 with 4 mmol of L1 and 1 g of ascorbic acid in 50 mL of ethanol for 6 h. Isolation and purification took place as described for the $[\text{Ru}(\text{bpy})_2(\text{L})]^{2+}$ complexes.

$[\text{Ru}(\text{L1})_3](\text{PF}_6)_2 \cdot \text{H}_2\text{O}$. Yield: 0.31 g (35%). Anal. Calcd for $\text{C}_{21}\text{H}_{23}\text{F}_{12}\text{N}_9\text{O}_2\text{P}_2\text{Ru}$: C, 28.3; H, 2.6; N, 23.5; P, 6.9. Found: C, 28.1; H, 2.6; N, 23.7; P, 7.0.

Results

Nuclear Magnetic Resonance. The ^1H NMR data obtained for the ruthenium bis(bipyridyl) pyrazinyltriazole complexes are summarized in Table II. In spite of the complexity of the spectra, it was possible to assign most of the peaks by using two-dimensional COSY NMR, as illustrated in Figure 2. However, no full assignment has been given. The triazole ring in the pyrazinyl-

(11) Delaby, R.; Damiens, R.; Robba, M. C. *R. Hebd. Seances Acad. Sci.* **1958**, *247*, 822.

(12) Kubota, S.; Uda, M.; Nakagawa, T. *J. Heterocycl. Chem.* **1975**, *12*, 855.

(13) Kubota, S.; Uda, M.; Nakagawa, T. *J. Heterocycl. Chem.* **1975**, *12*, 855.

(14) Lin, Y.; Lang, S. A., Jr.; Lovell, M. F.; Perkinson, N. A. *J. Org. Chem.* **1979**, *44*, 4161.

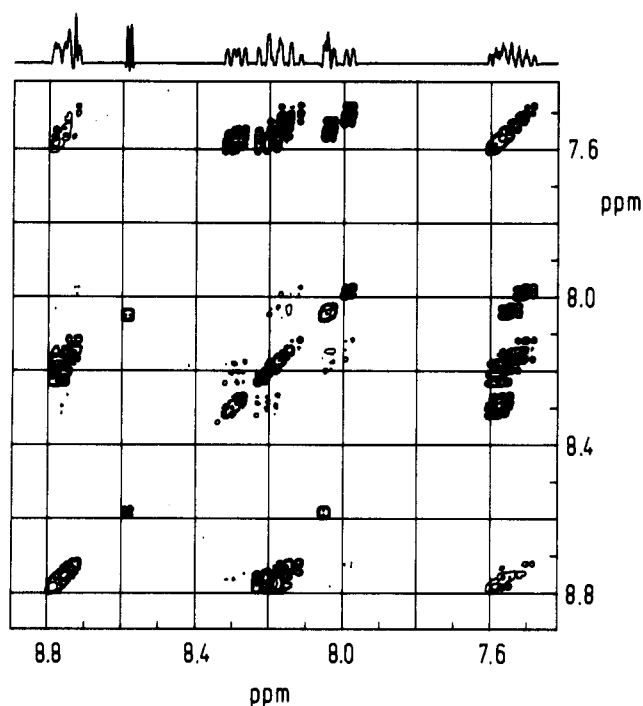
(15) Ross, H. B.; Boldaji, M.; Rillema, D. P.; Blanton, C. B.; White, R. P. *Inorg. Chem.* **1989**, *28*, 1013.

(16) Sullivan, B. P.; Salmon, D. J.; Meyer, T. J. *Inorg. Chem.* **1978**, *17*, 3334.

Table II. ^1H NMR Chemical Shifts of the Pyrazinyltriazole Protons in ppm Relative to TMS ($(\text{CD}_3)_2\text{CO}$)^a

compd	H ₃	H ₅	H ₆	H _{5'}	CH ₃
[Ru(bpy) ₂ (L0)] ⁺	9.26	7.89	8.31	8.01	
	(-0.20)	(-0.81)	(-0.35)	(-0.24)	
[Ru(bpy) ₂ (HL0)] ²⁺	9.59	7.95	8.60	8.91	
	(+0.13)	(-0.75)	(-0.06)	(+0.66)	
[Ru(bpy) ₂ (L1)] ²⁺	9.47	8.06	8.60	8.75	4.10
	(+0.08)	(-0.63)	(-0.02)	(+0.53)	(+0.04)
[Ru(bpy) ₂ (L2)] ²⁺	9.79	8.27	8.67	8.26	4.57
	(+0.50)	(-0.53)	(+0.10)	(+0.14)	(+0.34)
[Ru(bpy) ₂ (L3)] ⁺	9.18	7.80	8.24	2.25	
	(-0.02)	(-0.91)	(-0.53)		(-0.16)
[Ru(bpy) ₂ (HL3)] ²⁺	9.37	8.05	8.51	2.48	
	(+0.17)	(-0.34)	(-0.16)		(+0.07)
[Ru(L1) ₃] ²⁺	9.44	8.34	8.55	8.77 ^b	4.09 ^b
	9.46	8.43	8.63	8.82 ^c	4.10 ^c
				8.87 ^c	4.12 ^c
				8.95 ^c	

^aThe values in parentheses are the changes in chemical shifts compared to the free ligands. ^b*fac* isomer. ^c*mer* isomer.

**Figure 2.** COSY ^1H NMR spectrum of $[\text{Ru}(\text{bpy})_2(\text{L1})]^{2+}$.

triazole ligands and the previously reported pyridyltriazole ligands can bind in two ways, via N2' or via N4' of the triazole ring.¹⁰ By comparison of the chemical shifts of the coordinated ligands with those of the free ligand and by use of space-filling models, the coordination mode of the pyrazinyltriazole ligands has been determined.

The chemical shifts of the protons of the ligands are influenced by three factors:¹⁷ (i) the electron density on the ligands diminishes upon coordination, inducing a downfield shift; (ii) steric effects lead to a downfield shift; (iii) alignment of a proton above an adjacent aromatic ring leads to a dramatic upfield shift. An example of steric effects can be observed for $[\text{Ru}(\text{bpy})_2(\text{L2})]^{2+}$, where the triazole methyl group is close to the H3 proton of the pyrazine ring, leading to a substantial downfield shift for both H3 and the protons of the methyl group (see Table II).

For steric reasons it is expected that L1 and also L2 coordinate through N4'. Space-filling models show that when L1 is coordinated through N4', the methyl group is completely free and has no interactions with other ligands. However, when bound through N2', the methyl group is close to one of the bpy ligands and a large upfield magnetic shift is expected for the methyl group compared to the free ligand.¹⁷ The NMR data show no significant

Table III. UV-Vis Absorption and Emission Data and Lifetimes of Ruthenium Pyrazinyltriazole and Related Compounds

no.	compd	absorption (300 K) λ_{max} nm (ϵ , $10^4 \text{ M}^{-1} \text{ cm}^{-1}$)	emission λ_{max} nm (τ , μs)	
			77 K ^a	300 K ^b
1	[Ru(bpy) ₂ (HL0)] ²⁺	440 (1.32)	612 (4.9)	662 (0.10)
2	[Ru(bpy) ₂ (L0)] ⁺	456 (1.14)	618 (4.1)	680 (0.08)
3	[Ru(bpy) ₂ (L1)] ²⁺	440 (1.45)	575 (7.8)	630 (0.07)
4	[Ru(bpy) ₂ (L2)] ²⁺	443 (1.38)	577 (7.8)	680 (0.19)
5	[Ru(bpy) ₂ (HL3)] ²⁺	441 (1.27)	620 (5.2)	665 (0.14)
6	[Ru(bpy) ₂ (L3)] ⁺	458 (1.21)	627 (3.8)	670 (0.07)
7	[Ru(L1) ₃] ²⁺	417 (1.47)	574 (6.3)	600
8	[Ru(bpy) ₃] ²⁺	452 (1.30)	582 (4.8)	615 (0.8) ^c
9	[Ru(bpz) ₃] ²⁺	440 (1.30)	573	610 (0.74) ^{c,d}
10	[Ru(bpy) ₂ (bpz)] ²⁺	473 (0.99)	639 (3.4)	710 (0.38) ^{c,d}
11	[Ru(bpm) ₃] ²⁺	454 (0.86)	588	639 (0.13) ^d
12	[Ru(bpy) ₂ (bpm)] ²⁺	480		710 (0.08) ^d

^a Measured in propionitrile/butyronitrile (4/5 v/v). ^b Measured in acetonitrile at a concentration of 10^{-5} M. ^c Reference 3. ^d References 23 and 24.

shift of the methyl group, which indicates that L1 indeed coordinates via N4' of the triazole ring. This conclusion is in agreement with previous X-ray studies of ruthenium complexes with the analogous 1-methylpyridyltriazole ligand.^{18,19}

By comparison of the data for the free ligand HL3 and the coordinated one, it can be seen that the chemical shift of the methyl group hardly changes. This suggests, if arguments similar to those given above are used, that the ligand binds through N2' and not through N4'. The same coordination mode also has been observed previously for $[\text{Ru}(\text{bpy})_2(3\text{-methyl-5-(2-pyridyl)-1,2,4-triazole})]\text{PF}_6 \cdot 4\text{H}_2\text{O}$.²⁰

For HL0 the situation is more complicated, because for this ligand the two coordination modes (N2' or N4') are from steric considerations identical. Inspection of the NMR spectrum of $[\text{Ru}(\text{bpy})_2(\text{L0})]^{+}$ shows that for the sample obtained only one H5' signal is present at 8.01 ppm, which is 0.24 ppm to higher field than the chemical shift of this proton in the free ligand. Similarly, for the complex containing protonated HL0, also only one H5' resonances at 8.91 ppm (+0.66) is observed. This is indicative for the presence of only one coordination isomer, with either N2' or N4' coordination. Also HPLC experiments suggest that only one isomer is present. However, as mentioned in the Experimental Section for $[\text{Ru}(\text{bpy})_2(\text{L0})]\text{PF}_6 \cdot \text{H}_2\text{O}$, a yield of only 30% was obtained. This low yield might indicate that one geometrical isomer precipitates preferentially. The other isomer has so far not been isolated, but HPLC analysis of a second fraction strongly suggests the presence of a second isomer in a low yield.²¹

We are currently trying to separate both isomers for further studies. For the analogous pyridyltriazole complexes, the two geometrical isomers (N2' and N4') have recently been separated and the NMR spectra of both isomers have been obtained.²⁰ For the deprotonated-N2'-coordinated isomer an upfield shift of 0.28 ppm and for the N4'-bound isomer an upfield shift of 0.77 ppm have been observed.²⁰ The small upfield shift of the H5' proton in $[\text{Ru}(\text{bpy})_2(\text{L0})]^{+}$ suggests that the isolated complex contains pyrazinyltriazole that is coordinated via N2' to the ruthenium center. The small upfield shift of the H5' proton could be caused by the negative charge of the triazolate ligand, which causes a general upfield shift of the protons.

From the NMR experiments it is therefore concluded that in the compound isolated the ligands L1 and L2 are bound via N4',

- (17) Steel, P. J.; Lahousse, F.; Lerner, D.; Marzin, C. *Inorg. Chem.* **1983**, *22*, 1488.
- (18) Forster, R. J.; Boyle, A.; Vos, J. G.; Hage, R.; Dijkhuis, A. H. J.; Graaff, R. A. G.; Haasnoot, J. G.; Reedijk, J. *J. Chem. Soc., Dalton Trans.* **1990**, 121.
- (19) Hage, R.; Prins, R.; de Graaff, R. A. G.; Haasnoot, J. G.; Reedijk, J.; Vos, J. G. *Acta Crystallogr., Sect. C* **1988**, *C44*, 56.
- (20) Buchanan, B. E.; Vos, J. G.; van der Putten, W. J. M.; Kelly, J. M.; Hage, R.; de Graaff, R. A. G.; Prins, R.; Haasnoot, J. G.; Reedijk, J. *J. Chem. Soc., Dalton Trans.* **1990**, 2425.
- (21) Buchanan, B. E.; McGovern, E.; Harkin, P.; Vos, J. G. *Inorg. Chim. Acta* **1988**, *154*, 1.

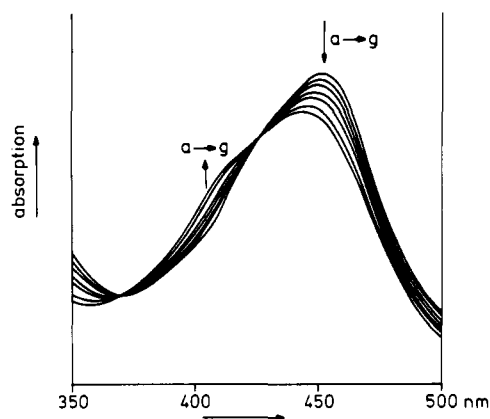


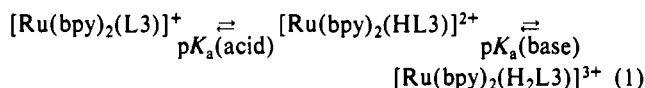
Figure 3. pH dependence of the absorption spectrum of $[\text{Ru}(\text{bpy})_2(\text{HL3})]^{2+}$ in an aqueous Britton-Robinson buffer. Key for curves a-h: (a) pH 6.71; (b) 5.25; (c) 4.79; (d) 4.34; (e) 4.09; (f) 3.87; (g) 2.14.

while HL0 and HL3 are coordinated via N2' of the triazole ring to the $\text{Ru}(\text{bpy})_2$ moiety.

UV-Vis Absorption Spectroscopy and Ground-State Acid-Base Chemistry. The UV-vis absorption and electrochemical data of ruthenium bis(pyridyl) complexes are summarized in Table III.

In the UV-vis absorption spectra one broad band is observed in the visible part of the spectrum at about 440–455 nm, as illustrated in Figure 3. By comparison with literature data this band can be assigned to $d\pi-\pi$ metal-to-ligand charge-transfer (MLCT) transitions.³

The acid-base chemistry of the compounds was investigated by using UV-vis absorption spectroscopy. The removal of the triazole-based proton ($\text{p}K_a(\text{acid})$) in HL0 and HL3 causes a rather small red shift of about 15 nm in the absorption maxima. A typical titration plot is given in Figure 3. The $\text{p}K_a(\text{acid})$ values obtained for the complexes are 3.1 for $[\text{Ru}(\text{bpy})_2(\text{HL0})]^{2+}$ and 4.2 for $[\text{Ru}(\text{bpy})_2(\text{HL3})]^{2+}$.



The ruthenium compounds can also be protonated on the non-coordinating nitrogen of the pyrazine ring in concentrated sulfuric acid ($\text{p}K_a(\text{base})$ in eq 1), as has been shown previously by Crutchley et al. for bipyrazine-containing compounds.⁷

The ruthenium bis(bipyridyl) pyrazinyltriazole compounds were stable in strong acidic media. Even from 96% sulfuric acid they could be recovered unchanged after neutralization. For increasing Hammett acidity ($-H_0$) values²² the major absorption peak (around 450 nm) in the UV-vis spectrum decreases, while two new absorption bands show up at 400 and 530 nm. The $\text{p}K_a(\text{base})$ values for all complexes are -1.8 , and an example of a titration experiment is presented in Figure 4. The measured $\text{p}K_a(\text{base})$ values for the complexes are similar to the value obtained by Crutchley et al. for $[\text{Ru}(\text{bpz})_3]^{2+}$ ($\text{p}K_a(\text{base}) = -2.2$).⁷

Emission Spectroscopy. The emission properties of the pyrazinyltriazole-containing ruthenium complexes have been listed in Table III. Also some data of analogous complexes containing 2,2'-bipyrazine (bpz) and 2,2'-bipyrimidine (bpm) have been added. $[\text{Ru}(\text{L1})_3]^{2+}$ exhibits a strong emission with a rather long lifetime at 77 K. At room temperature, the emission has nearly disappeared and no lifetime could be obtained. A similar, although less pronounced, effect has been observed for $[\text{Ru}(\text{bpz})_3]^{2+}$ and $[\text{Ru}(\text{bpm})_3]^{2+}$ and a detailed analysis has revealed that population of strongly deactivating ³MC states causes a strong decrease of the luminescence lifetime at room temperature.²³⁻²⁵ For the

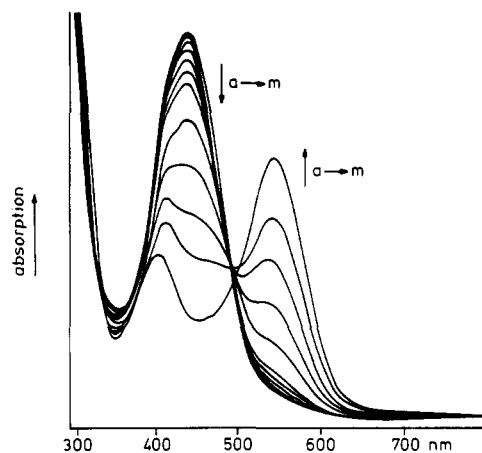


Figure 4. Titration of $[\text{Ru}(\text{bpy})_2(\text{L1})]^{2+}$ with sulfuric acid. Key for $-H_0$ values of curves a-m: (a) -7.00 ; (b) -0.70 ; (c) -0.42 ; (d) -0.12 ; (e) 0.10 ; (f) 0.30 ; (g) 0.43 ; (h) 0.72 ; (i) 1.13 ; (j) 1.50 ; (k) 2.10 ; (l) 2.58 ; (m) 3.14 .

Table IV. Electrochemical Data for the Compounds^a

no.	compd	oxidn pot.	redn pot.	$\Delta E_{1/2}$
1	$[\text{Ru}(\text{bpy})_2(\text{HL0})]^{2+}$	1.30	$-1.23, -1.53, -1.78$	2.53
2	$[\text{Ru}(\text{bpy})_2(\text{L0})]^+$	0.95	$-1.44, -1.66, -1.96$	2.39
3	$[\text{Ru}(\text{bpy})_2(\text{L1})]^{2+}$	1.30	$-1.26, -1.52, -1.77$	2.56
4	$[\text{Ru}(\text{bpy})_2(\text{L2})]^{2+}$	1.31	$-1.09, -1.51, -1.77$	2.40
5	$[\text{Ru}(\text{bpy})_2(\text{HL3})]^{2+}$	1.29	$-1.22, -1.52, -1.77$	2.51
6	$[\text{Ru}(\text{bpy})_2(\text{L3})]^+$	0.92	$-1.44, -1.66, -1.80$	2.36
7	$[\text{Ru}(\text{L1})_3]^{2+}$	1.40	$-1.25, -1.46, -1.76$	2.65
8	$[\text{Ru}(\text{bpy})_3]^{2+}$	1.23	$-1.36, -1.54, -1.79$	2.59
9	$[\text{Ru}(\text{bpz})_3]^{2+}$	1.93	$-0.74, -0.92, -1.18$	2.67

^a Measured in CH_3CN with 0.1 M TBAP. Potentials in V versus SCE. $\Delta E_{1/2} (\text{V}) = E_{\text{ox}} - E_{\text{red}}$.

mixed-ligand chelate complexes, the ³MC states are not populated at room temperature and only ³MLCT states play a role in the temperature dependency of the lifetimes. Although no detailed analysis has been carried out on the $[\text{Ru}(\text{bpy})_2(\text{L})]^{2+}$ systems, it is likely that the same kind of processes govern the photophysical properties of the pyrazinyltriazole systems.

The complexes with HL0 and HL3 have at 77 K emission maxima at lower energy than the complexes containing L1 and L2. This difference in emission energy could be caused by the different coordination modes of HL0, HL3 (N2'), and L1 and L2 (N4'). Surprisingly, deprotonation of HL0 and HL3 causes only a very small shift in the emission energy, but the lifetimes of $[\text{Ru}(\text{bpy})_2(\text{L0})]^+$ and $[\text{Ru}(\text{bpy})_2(\text{L3})]^+$ are significantly shorter than those found for the protonated species. A possible explanation for this behavior will be given in the Discussion.

When the pyrazine ring is protonated with concentrated sulfuric acid, the compounds show no emission.

Electrochemistry. Both differential-pulse polarography and cyclic voltammetry have been applied to study the redox properties of the ruthenium compounds reported here. It should be noted that it was difficult to obtain accurate values for the reduction potentials of the compounds containing neutral HL0 and HL3 in the acidified solutions.

The complexes with L1, L2, HL0, and HL3 are much alike in redox behavior (Table IV). As shown in Table IV, deprotonation of HL0- and HL3-containing compounds influences the electrochemical data as well as absorption and emission properties, as described previously (Figure 5). The oxidation potentials of complexes with deprotonated ligands L0⁻ and L3⁻ are significantly less positive than those of the other complexes, while the reduction potentials are more negative for $[\text{Ru}(\text{bpy})_2(\text{L0})]^+$ and $[\text{Ru}(\text{bpy})_2(\text{L3})]^+$ than for the other complexes.

Upon protonation of the pyrazine rings of the ligands of the various complexes, the oxidation potentials are shifted by about 150 mV to higher potentials. The reduction potentials could not

(22) Long, F. A.; Paul, M. A. *Chem. Rev.* **1957**, *57*, 1.

(23) Allan, G. H.; White, R. P.; Rillema, D. P.; Meyer, T. J. *J. Am. Chem. Soc.* **1984**, *106*, 2613.

(24) Rillema, D. P.; Allen, G.; Meyer, T. J.; Conrad, D. *Inorg. Chem.* **1983**, *22*, 1618.

(25) We would like to thank one of the reviewers pointing out this fact.

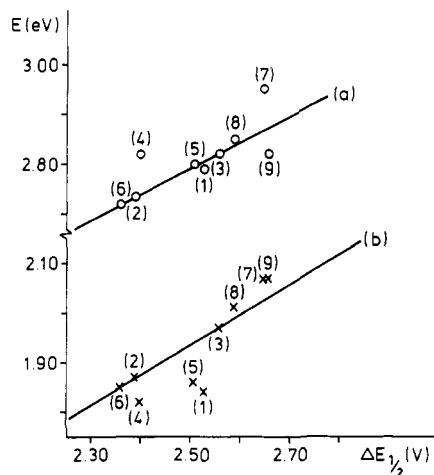


Figure 5. Plots of $\Delta E_{1/2}$ versus (a) absorption and (b) emission energies for compounds 1–9 (see Table III for numbering of compounds).

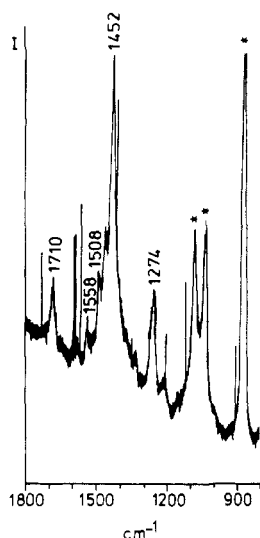


Figure 6. Resonance Raman spectrum of $[\text{Ru}(\text{L}1)_3]^{2+}$, excited with 458 nm in acetonitrile. Bands marked with an asterisk are solvent bands.

be measured in these strongly acidic solutions.

Resonance Raman Measurements. Resonance Raman (rR) spectra can be used for the assignment of the nature and characterization of electronic transitions.^{26–28} If excitation takes place into an allowed electronic transition, the rR spectrum is characterized by strong rR effects for the vibrations of those bonds that are mostly affected by the electronic transition. Thus, excitation into an allowed $\text{Ru} \rightarrow \pi^*(\alpha\text{-diimine})$ transition primarily affects the diimine bonds. As a result, enhancement of Raman intensity is normally observed for the symmetrical stretching modes of the α -diimine ligand. With this method also the presence of different electronic transitions within one absorption band can be detected and identified by studying the wavelength dependence of the rR spectra.²⁹

Figure 6 presents the rR spectrum of $[\text{Ru}(\text{L}1)_3]^{2+}$ obtained by excitation with a wavelength of 458 nm. Comparison with the corresponding spectra of $[\text{Ru}(\text{bpz})_3]^{2+}$ revealed that the enhanced bands at 1710, 1558, 1508, 1452, and 1274 cm^{-1} are pyrazine-based vibrations.^{30,31} No strong triazole vibrations were observed

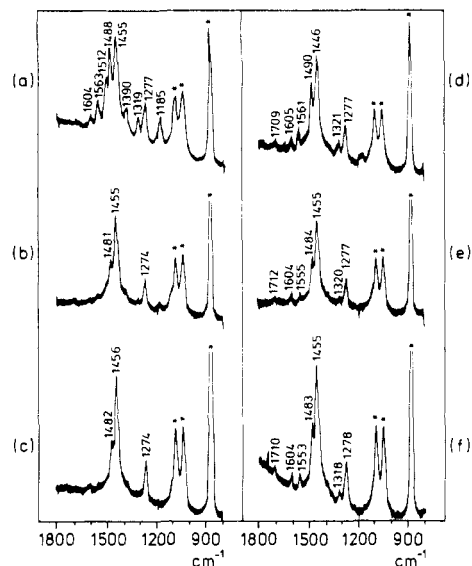


Figure 7. Resonance Raman spectra of $[\text{Ru}(\text{bpy})_2(\text{HL}3)](\text{PF}_6)_2$, excited with (a) 458, (b) 488, and (c) 514.5 nm, and $[\text{Ru}(\text{bpy})_2(\text{L}3)](\text{PF}_6)_2$, excited with (d) 458, (e) 488, and (f) 514.5 nm, in acetonitrile. Bands marked with an asterisk are solvent bands.

in the rR spectrum. This indicates that after excitation most of the negative charge resides at the pyrazine ring.

Excitation of $[\text{Ru}(\text{bpy})_2(\text{L}1)]^{2+}$, $[\text{Ru}(\text{bpy})_2(\text{L}2)]^{2+}$, and $[\text{Ru}(\text{bpy})_2(\text{HL}3)]^{2+}$ with a wavelength of 514.5 nm yielded rR spectra that are very similar to those observed for $[\text{Ru}(\text{L}1)_3]^{2+}$, with intensity enhancement at 1720, 1558, 1512, 1455, and 1277 cm^{-1} . After excitation with 488 nm, again mainly pyrazinyltriazole vibrations were visible, but after excitation with 458 nm bpy vibrations at 1603, 1559, 1489, 1319, and 1185 cm^{-1} were observed for these complexes.³² As a representative example, Figure 7 shows the rR spectra of $[\text{Ru}(\text{bpy})_2(\text{HL}3)]^{2+}$ at different wavelengths of excitation. From these spectra it can be concluded that the low-energy sides of the MLCT bands of these complexes belong to one or more $d\pi \rightarrow \pi^*(\text{L})$ transitions and that the $d\pi \rightarrow \pi^*(\text{bpy})$ transitions become apparent at the high-energy sides.

The same conclusion was drawn for the $[\text{Ru}(\text{bpy})_2(\text{bpz})]^{2+}$ dication; low-energy excitation yielded a rR spectrum with only bpz vibrations, whereas upon excitation with 458 nm, also bpy vibrations became visible.³²

The rR spectra of $[\text{Ru}(\text{bpy})_2(\text{L}3)]^+$ are also presented in Figure 7. Again, after excitation with 458 nm, resonance-enhanced bpy and pyrazinyltriazole vibrations are visible. However, upon excitation with 488 nm, the bpy vibrations are still clearly visible, and even after excitation with 514.5 nm, the rR spectrum has hardly changed. This indicates that the overlap between the $d\pi \rightarrow \pi^*(\text{bpy})$ and a $d\pi \rightarrow \pi^*(\text{L}3)$ transitions in the absorption spectrum of $[\text{Ru}(\text{bpy})_2(\text{L}3)]^+$ is much larger than in the case of the protonated species.

RR spectra were also recorded for the complexes dissolved in a solution of 20% H_2SO_4 in ethanol. The spectra excited with 514.5 nm only showed vibrations of the pyrazinyltriazole ligands and not those of bpy (Figure 8). Excitation with 458 nm shows also some bpy vibrations, which indicates that both $d\pi \rightarrow \pi^*(\text{L})$ and $d\pi \rightarrow \pi^*(\text{bpy})$ transitions are present (Figure 8). These results indicate that low-energy bands in the absorption spectra of the complexes reported in 20% H_2SO_4 originate from a $d\pi \rightarrow \pi^*(\text{L})$ transition, while the band at 400 nm is due to a $d\pi \rightarrow \pi^*(\text{bpy})$ transition.

Discussion

It has previously been noted that the photophysical properties of $[\text{Ru}(\text{bpy})_2(\text{LL}')^{2+}$ ($\text{LL}' =$ various substituted pyridyltriazoles)

- (26) Basu, A.; Gafney, H. D.; Streckas, T. C. *Inorg. Chem.* **1982**, *21*, 2231.
 (27) Braunstein, C. H.; Baker, A. D.; Streckas, T. C.; Gafney, H. D. *Inorg. Chem.* **1984**, *23*, 857.
 (28) Stufkens, D. J.; Snoeck, T. L.; Lever, A. B. P. *Inorg. Chem.* **1988**, *27*, 953.
 (29) Servaas, P. C.; van Dijk, H. K.; Snoeck, T. L.; Stufkens, D. J.; Oskam, A. *Inorg. Chem.* **1985**, *23*, 4494.
 (30) Balk, W.; Stufkens, D. J.; Crutchley, R. J.; Lever, A. B. P. *Inorg. Chim. Acta* **1982**, *64*, L49.

- (31) Toma, H. E.; Santos, P. S.; Lever, A. B. P. *Inorg. Chem.* **1988**, *27*, 3850.
 (32) Tait, C. D.; Donohoe, R. J.; DeArmond, M. K.; Wertz, D. W. *Inorg. Chem.* **1987**, *26*, 2754.

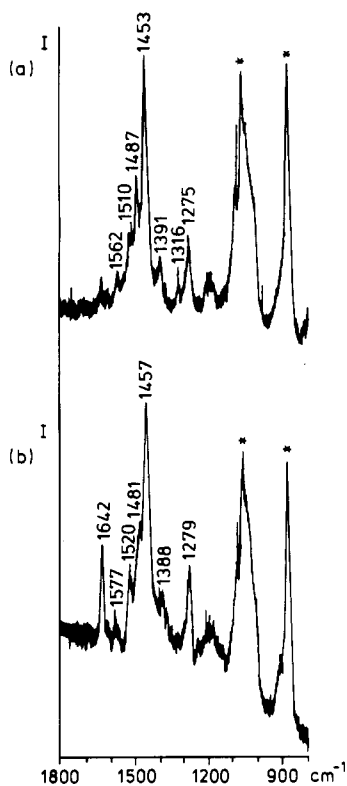


Figure 8. Resonance Raman spectra of $[\text{Ru}(\text{bpy})_2(\text{HL3})]^{3+}$, protonated in 20% H_2SO_4 in ethanol solution, excited with (a) 458 and (b) 514.5 nm. Bands marked with an asterisk are solvent bands.

are dominated by bpy-localized processes.⁵ Comparison of the properties of the free pyrazinyltriazole ligands with the analogous pyridyltriazole ligands²⁰ shows a number of interesting features.

(i) The free HL0 and HL3 ligands have slightly lower $pK_a(\text{acid})$ values (8.7 and 9.4) than their pyridyltriazole analogues (9.2 and 9.8). Also the $pK_a(\text{acid})$ values of the coordinated HL0 and HL3 ligands (3.1 and 4.2) are lower than observed for the analogous bound pyridyltriazole ligands (4.1 and 4.9).²⁰ These differences suggest that the pyrazinyltriazole are weaker σ -donor ligands than their pyridyltriazole analogues. In general ligands with high $pK_a(\text{acid})$ values are strong σ -donor ligands and weaker π -accepting ligands.³³

(ii) The higher $pK_a(\text{acid})$ values of HL0 and HL3 indicate that L0^- and L3^- have stronger σ -donor properties than bpy, which has a $pK_a(\text{base})$ of 4.4.³³⁻³⁵ It is therefore expected that the deprotonated ligands are more difficult to be reduced than bpy. The same observation has been made for the pyridyltriazole ligands.

(iii) Finally, the reduction potentials of the free neutral ligands are less negative than that observed for bpy (-2.21 V vs SCE³⁷), and those of the analogous pyridyltriazole ligands,²⁰ suggesting that the pyrazinyltriazole ligands are better π -acceptor ligands than bpy and the pyridyltriazoles.

The first reduction potentials of $[\text{Ru}(\text{bpy})_2(\text{HL0})]^{2+}$, $[\text{Ru}(\text{bpy})_2(\text{L1})]^{2+}$, $[\text{Ru}(\text{bpy})_2(\text{L2})]^{2+}$, and $[\text{Ru}(\text{bpy})_2(\text{HL3})]^{2+}$ are less negative than the first reduction potential of $[\text{Ru}(\text{bpy})_3]^{2+}$ (Table IV). This suggests that in these compounds the first reduction potential is pyrazinyltriazole based, especially since from the electrochemical measurements on the free ligands, the HL0, L1, L2, and HL3 ligands are expected to be better π -acceptor ligands than bpy (Table I). The oxidation potentials of $[\text{Ru}(\text{bpy})_2(\text{HL0})]^{2+}$, $[\text{Ru}(\text{bpy})_2(\text{L1})]^{2+}$, $[\text{Ru}(\text{bpy})_2(\text{L2})]^{2+}$, and $[\text{Ru}(\text{bpy})_2(\text{HL3})]^{2+}$ are 100 mV higher than found for the pyridyltriazole-containing complexes, indicating that the pyrazinyltriazole ligands are somewhat weaker σ -donor ligands than the pyridyltriazole ligands. The nature of the enhanced vibrations in the rR measurements suggests that the low-energy side of the absorption band has mainly pyrazinyltriazole character, while the high-energy side of the transition appears to be bpy based.

Deprotonation of $[\text{Ru}(\text{bpy})_2(\text{HL3})]^{2+}$ and $[\text{Ru}(\text{bpy})_2(\text{HL0})]^{2+}$ causes changes in the electrochemical potentials and absorption, emission, and rR spectra (Tables III and IV). The oxidation potential is lowered because, after deprotonation, the triazole ligands are better σ -donor ligands,⁵ with the result that more charge is present at the metal ion. The oxidation potentials of the deprotonated species are about 100 mV higher than the analogous pyridyltriazole complexes, again indicating that the σ -donor properties of the pyrazinyltriazoles are weaker than the pyridyltriazoles.

In the compounds containing deprotonated L0^- and L3^- , the first reduction wave is most likely bpy based instead of pyrazinyltriazole based. This can be substantiated for the following three reasons. First, the reduction potentials are very similar to those of $[\text{Ru}(\text{bpy})_2(\text{pyridyltriazole})]^{2+}$, for which already was concluded that a first bpy-based reduction is present.⁵ Second, the $pK_a(\text{acid})$ measurements of HL0 and HL3 indicated that the σ -donor properties of L0^- and L3^- are stronger than those of bpy. Furthermore, the negative charge on the deprotonated pyrazinyltriazole ligands makes it very likely that the first reduction is occurring at the bpy ligand. Third, the rR measurements indicate that much more bpy character is present at the low-energy side of the MLCT band, indicating that, compared to the protonated species, the bpy-based π^* level is lowered with respect to the π^* level of the pyrazinyltriazole ligands.

So, by comparison of UV-vis absorption and electrochemical data two categories of ruthenium bis(bipyridyl) pyrazinyltriazole complexes can be distinguished, in which the first reduction potential is either bpy based, as for deprotonated L0^- and L3^- , or pyrazinyltriazole based, as for the complexes with HL0, L1, L2, and HL3.

As absorption is a $d\pi \rightarrow \pi^*$ process to the single MLCT state, and a relation between the energy difference in the ¹MLCT and ³MLCT states has been observed before for other ruthenium(II) systems,^{3,36,37} it is likely that the location of the emitting state for the pyrazinyltriazole-containing complexes is related to the nature of the ¹MLCT state. Because the electrochemical and resonance Raman experiments revealed that the first reduction potentials of $[\text{Ru}(\text{bpy})_2(\text{L})]^{2+}$ (L = HL0, L1, L2, and HL3) are pyrazinyltriazole based and the lowest MLCT band is a $d\pi \rightarrow \pi^*(\text{L})$ transition, it is very likely that the emission of the mixed-ligand complexes with HL0, L1, L2, and HL3 are pyrazinyltriazole based. Also the similar lifetimes and emission energies of $[\text{Ru}(\text{L1})_3]^{2+}$ and $[\text{Ru}(\text{bpy})_2(\text{L})]^{2+}$ suggest that the emitting states in both complexes are the same and therefore L1 based.

Deprotonation of the complexes containing HL0 and HL3 causes a change in the nature of the MLCT band (more bpy character), and the first reduction potential is now bpy based. It is therefore anticipated that the emission originates from one of the bpy ligands and not from the L ligands. More detailed experiments are, however, necessary to fully reveal the emission properties of these complexes.

As shown in Figure 5, a distinct relationship exists between the absorption/emission maxima and the difference in oxidation and reduction potentials for the pyrazinyltriazole complexes. Relationships between the redox potentials and the absorption/emission maxima have been observed previously by different groups. The energy of absorption and emission MLCT transitions is related to the electrochemical potentials as given in eqs 2 and 3,^{3,36,37} where

$$h\nu^{\text{abs}} = \Delta E_{1/2} + A \quad (2)$$

$$h\nu^{\text{em}} = \Delta E_{1/2} + B \quad (3)$$

$h\nu^{\text{abs}}$ = absorption energy, $h\nu^{\text{em}}$ = emission energy, $\Delta E_{1/2}$ =

(33) Ernst, S. D.; Kaim, W. *Inorg. Chem.* **1989**, *28*, 1520.

(34) Nakamoto, K. *J. Phys. Chem.* **1960**, *64*, 420.

(35) Barigelletti, F.; De Cola, L.; Balzani, V.; Hage, R.; Haasnoot, J. G.; Reedijk, J.; Vos, J. G. *Inorg. Chem.* **1989**, *28*, 4344.

(36) Dodsworth, E. S.; Lever, A. B. P. *Chem. Phys. Lett.* **1986**, *124*, 152.

(37) Barigelletti, F.; Juris, A.; Balzani, V.; Belser, P.; von Zelewsky, A. *Inorg. Chem.* **1987**, *26*, 4115.

$e[E_{1/2}(\text{ox}) - E_{1/2}(\text{red})]$, $E_{1/2}(\text{ox})$ and $E_{1/2}(\text{red})$ are the oxidation and reduction potentials of the complex, and A and B are terms that correct for the solvation energies, inner- and outer-sphere barriers, and Coulombic energies. The relationship between the absorption/emission maxima and the electrochemical potentials shows that the redox and spectroscopic orbitals are the same.

Protonation of the pyrazine ring causes a decrease in energy of the $d\pi-\pi^*$ transitions. Resonance Raman measurements have revealed that the low-energy band at 530 nm belongs to a $d\pi \rightarrow \pi^*$ (pyrazinyltriazole) transition, while the band at 400 nm is due to a $d\pi \rightarrow \pi^*$ (bpy) transition. Protonation of the free nitrogen in the pyrazine ring causes a stabilization of the π^* orbital.⁷ This will cause a more efficient π back-bonding from the ruthenium ion to the ligand. The electrochemical measurements indicate that after protonation of the pyrazine ring the ligand becomes a stronger π -acceptor² and a weaker σ -donor ligand. Less electron density is present on the ruthenium ion, and it is more difficult to oxidize the protonated complex.

There are two possible explanations why no emission is observed for the complexes in sulfuric acid: the emission maxima were present at lower energy than could be measured with our equipment (800 nm was the low-energy limit) or the complexes with a protonated pyrazine ring do not emit at all. This is unlike ruthenium compounds with bipyrazine and tetraazaphenanthrene, which are still emitting compounds after protonation.^{7,9} The weaker σ -donor capacities of the protonated pyrazinyltriazole ligand cause a decrease in the ligand field strength, and a lower ³MC state is expected. Therefore, a decrease in the quantum yield of the emission is observed.³

Conclusions. The electrochemical and spectroscopic data obtained for the ruthenium compounds containing the pyrazinyltriazole ligands HL0, L1, L2, and HL3 clearly indicate that in the complexes the LUMO's of the pyrazinyltriazole ligands are lower than the LUMO of bpy. Upon deprotonation of the complexes with HL0 and HL3, the LUMO of the compounds are now located on the bpy ligands. The emission data (energies and lifetimes) indicate that in $[\text{Ru}(\text{bpy})_2(\text{L})]^{2+}$ (L = HL0, L1, L2, and HL3) the pyrazinyltriazole ligands are most likely involved in the emission process, whereas the emission of $[\text{Ru}(\text{bpy})_2(\text{L}0^-)]^+$

and $[\text{Ru}(\text{bpy})_2(\text{L}3^-)]^+$ is bpy based.

Up till now, two types of acid–base behavior have been described for ruthenium(II) compounds. Class a compounds show a red shift of the absorption and emission maxima upon protonation of the coordinating ligands. Examples are ruthenium complexes with 2,2'-bipyrazine,⁷ 2,3-bis(2-pyridyl)pyrazine,³⁸ [4,7]-phenanthroline[5,6-*b*]pyrazine,³⁸ and 1,4,5,8-tetraazaphenanthrene.⁹ This red shift upon protonation of the ligands has been explained by stabilization of the π^* orbital.

The absorption and emission spectra of class b compounds are blue-shifted when protonated. Examples are $\text{Ru}(\text{bpy})_2$ complexes with imidazole^{38,39} pyrazole,¹⁶ and 1,2,4-triazole^{5,10} anions. Upon protonation of the ligands, less electron density is present at the metal center and therefore the filled $d\pi$ orbital is stabilized. This results in a larger energy difference between the $d\pi$ and the π^* orbitals.

A combination of above-mentioned effects is observed for the ruthenium complexes with the L0⁻ and L3⁻ ligands; when protonated, the filled $d\pi$ orbitals, as well as the π^* level of the pyrazinyltriazole ligand, are lowered. After protonation, the pyrazinyltriazole π^* orbital becomes just lower than the π^* orbital of bpy. Therefore, a combination of a higher oxidation potential and a less negative reduction potential is observed. This causes a rather small energy difference between the protonated and deprotonated species, which is reflected in the energies of the absorption and emission spectra of the protonated and deprotonated complexes.

Acknowledgment. We thank Johnson Matthey Chemical Ltd. (Reading, U.K.) for their generous loan of RuCl_3 . We wish to thank Unilever Research Laboratories (Vlaardingen, The Netherlands) for the use of the electrochemical equipment. Part of the emission measurements were performed in Bologna, Italy, during a stay of R.H. Dr. F. Barigelletti, Prof. V. Balzani, and Dr. L. De Cola are thanked for useful discussions.

(38) Hosek, W.; Tysoe, S. A.; Gafney, H. D.; Baker, A. D.; Strekas, T. C. *Inorg. Chem.* **1989**, *28*, 1228.

(39) Haga, M. *Inorg. Chim. Acta* **1983**, *75*, 29.

Contribution from the Departamento de Quimica Fisica, Facultad de Quimica, Universidad de Barcelona, 08028-Barcelona, Spain, Department of Chemistry, North Carolina State University, Raleigh, North Carolina 27695-8204, and Chemistry and Materials Science Divisions, Argonne National Laboratory, Argonne, Illinois 60439

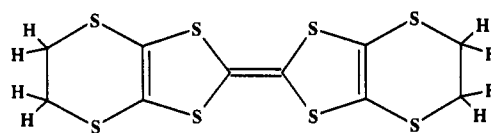
Interaction Energies Associated with Short Intermolecular Contacts of C–H Bonds. 1. Ab Initio Computational Study of C–H...Anion Interactions, C–H...X⁻ (X⁻ = I₃⁻, IBr₂⁻, ICl₂⁻)

Juan J. Novoa,*†‡ Fernando Mota,† Myung-Hwan Whangbo,*§ and Jack M. Williams*||

Received March 15, 1990

The nature of the C–H...anion contact interactions found for organic charge-transfer salts was investigated by performing SCF–MO and MP2 level calculations on the model systems $\text{H}_3\text{C–H}\cdots\text{Y–I–Y}^-$ (Y = I, Br, Cl). The binding energies of the $\text{H}_3\text{C–H}\cdots\text{Y–I–Y}^-$ systems are estimated to be 1.1, 1.3, and 1.6 kcal/mol for Y = I, Br, and Cl, respectively. The binding energy increase, observed when Y varies from I to Br to Cl, is consistent with the expected hydrogen-bonding abilities of the halogen atoms. The C–H bond prefers to make a short contact with the terminal halogen atoms of Y–I–Y⁻; this tendency increases as Y changes from I to Br to Cl, and the C–H...Y–I–Y⁻ interaction energies do not strongly depend upon the C–H...Y contact angle.

Organic donor molecules bis(ethylenedithio)tetrathiafulvalene (BEDT–TTF, **1**) and its analogues form 2:1 charge-transfer salts with a variety of monovalent anions X⁻.¹ Several BEDT–TTF salts are ambient-pressure superconductors, which include β -(BEDT–TTF)₂X (X⁻ = I₃⁻, AuI₂⁻, and IBr₂⁻, for which the su-



1

perconducting transition temperature $T_c = 1.4, 2.5, 3$ and 2.8 K,⁴ respectively) and κ -(BEDT–TTF)₂X (X⁻ = Cu(NCS)₂⁻ and I₃⁻,

*Universidad de Barcelona.

†On leave of absence at North Carolina State University.

‡North Carolina State University.

§Argonne National Laboratory.